

Poly (glycerol adipate) (PGA) Backbone Modifications with a Library of Functional Diols: Chemical and Physical Effects

Philippa L. Jacob,^a Laura A. Cantu Ruiz,^b Amanda K. Pearce,^c Yinfeng He,^b Joachim C. Lentz,^a Jonathan C. Moore,^a Fabricio Machado,^{a,d} Geoffrey Rivers,^b Edward Apebende,^a Maria Romero Fernandez,^a Iolanda Francolini,^e Ricky Wildman,^b Steven M. Howdle^a and Vincenzo Taresco^{a*}

- *School of Chemistry, University of Nottingham, University Park, NG7 2RD, Nottingham, United Kingdom*
- *Faculty of Engineering, University of Nottingham, University Park, Nottingham, NG7 2RD United Kingdom*
- *School of Chemistry, University of Birmingham, Birmingham, B15 2TT United Kingdom*
- *Laboratory of Chemical Processes Development, University of Brasília, Chemistry Institute, Campus Universitário Darcy Ribeiro, 70910-900 Brasília, DF, Brazil*
- *Department of Chemistry, Sapienza University of Rome, Piazzale Aldo Moro, 00185, Italy*

corresponding author: Vincenzo Taresco, email: vincenzo.taresco@nottingham.ac.uk

Abstract

Enzymatically synthesised poly(glycerol adipate) (PGA) has shown a palette of key desirable properties required for a biomaterial to be considered a ‘versatile polymeric tool’ in the field of drug delivery. PGA and its variations can self-assemble into nanoparticles (NPs) and interact at different levels with small active molecules. PGA derivatives are usually obtained by functionalising the glyceryl side hydroxyl group present along the main polymer scaffold. However, if the synthetic pathways are not finely tuned, the self-assembling ability of these new polymeric modifications might be hampered by the poor amphiphilic balance. For this reason, we have designed a straightforward one-pot synthetic modification, using a small library of diols in combination with glycerol, aimed at altering the backbone of the polymer without affecting the hydrophilic glyceryl portion. The diols introduce additional functionality into the backbone of PGA alongside the secondary hydroxyl group already present. We have investigated how extra functionalities along the polymer backbone alter the final polymer reactivity as well the chemical and biological properties of the nanoparticles. In addition, with the intent to further improve the green credentials of the enzymatic synthesis, a solvent derived from renewable resources, (2-methyl tetrahydrofuran, 2-MeTHF) was employed for the synthesis of all the PGA-variants as a replacement for the more traditionally used and fossil-based tetrahydrofuran (THF). *In vitro* assays carried out to evaluate the potential of these novel materials for drug delivery applications demonstrated very low cytotoxicity characteristic against NIH 3T3 model cell line.

Introduction

Glycerol is an untapped bio-renewable feedstock that is mainly produced as a by-product of biodiesel and bioethanol production^{1,2} and also the soap industry and crude oil.¹⁻³ The global production of this polyol has been predicted to exceed 4000 million litres by 2026.⁴ Glycerol is applied in a huge variety of industries such as food, cosmetics, tobacco and pharmaceuticals.² Despite this, the growing production of glycerol, mainly from the production of biodiesel is not matched by usage in other industrial sectors and, there is a need to develop new strategies for utilisation of this valuable resource through synthesis of glycerol-based polymers.

Glycerol can act as a monomer and will polymerise to yield both linear and highly branched polymers predominantly via step-growth mechanisms in combination with diacid monomers to synthesise poly(glycerol-diacid).⁵ The range of diacids, or derivatives, that have been polymerised with glycerol range from C₄ to C₁₄ aliphatic acids (e.g. sebacic acid, succinic acid, glutaric acid, suberic acid, azelaic acid and adipic acid)⁶⁻⁸ in addition to aromatic diacids and aliphatic-aromatic diacids.⁹ The polycondensation of glycerol with this palette of diacids can afford linear, branched and cross-linked materials according to the reaction conditions adopted (e.g. nature of solvent, comonomer and catalyst, reaction temperature).¹⁰⁻¹² In this regard, the chemo- and regioselectivity of lipases have enabled elegant, and adaptable production of linear glycerol-based polyesters under mild reaction conditions (different reaction media, low temperature and ambient pressure) preserving the secondary glyceryl hydroxyl moiety along the backbone of the resulting macromolecules.¹³ In this way, the available hydroxyl moiety gives rise to a polymer that can undergo a variety of further functionalisations *via* simple chemistry avoiding tedious and lengthy protection/deprotection intermediate steps.^{14,15}

In particular, the enzymatically catalysed reaction of glycerol and divinyl adipate (DVA) can produce poly(glycerol adipate) (PGA), a functionalisable, biocompatible (*in vitro* and *in vivo*) and biodegradable polymer.¹⁶⁻¹⁸ Furthermore, thanks to the chemical nature of its repetitive unit, PGA shows an amphiphilic balance capable of self-assembly into NPs in aqueous media, without the use of additional stabilizers.¹⁹ Based on this evidence, PGA is a promising functionalisable, (bio)degradable and (bio)compatible polymeric carrier ideal for drug delivery applications with enhanced chemical, physical and biological properties.^{16,20,21} To date, post-polymerization-functionalisation is the most common strategy to tailor the final properties of PGA and broaden its chemical diversity for specific applications. In fact, the free hydroxyl group of PGA has been coupled to a variety of molecules, with a wide range of chemical and biological properties (e.g. fatty acids, amino acids, drugs, etc.)²²⁻²⁷ in order to tune its ability to self-assemble into NPs for delivery of lipophilic and hydrophilic drugs as well as to produce polymeric active pro-drugs.²⁸⁻³⁴ However, if the degree of coupling is not controlled, according to the nature of the added functionalities, the unbalancing of the amphiphilic ratio and the loss of free hydroxyl moieties may negatively affect the self-assembling ability.

Others have performed one-pot enzymatic polycondensation/ring-opening polymerization (ROP) by adding pentadecalactone (PDL) to the initial DVA/glycerol mixture in order to modify the PGA backbone. The resultant PGA-co-PDL polymer showed different thermal properties and amphiphilicity when compared to the original PGA.^{35,36} PGA-co-PDL (and its

PEGylated variant) is one of the few, if not the only example of PGA backbone modification adopted for the encapsulation of small and large active molecules.^{37,38} With the intent to both preserve the glyceryl portion and broaden the range of chemistries added along the PGA backbone, in this paper we set out to design a straightforward one-pot synthetic modification, using a small library of diols in combination with glycerol and divinyl adipate. In particular, the glycerol moiety was partially replaced by the diols according to the functional groups involved, maintaining a 1:1 stoichiometry molar ratio (considering that only the primary alcohols of glycerol would react in the polycondensation step). The selected diols (ethylene glycol, PEG400, 1,4-butyne diol, 1,4-butanediol, 1,3-benzodimethanol, 2-hydroxyethyl disulfide and 1,6-hexanediol) may introduce either additional functionalities able to tune the amphiphilic balance of the final polymeric materials or functionalisable chemical handles directly into the backbone of PGA (alongside the secondary hydroxyl group already present). We aim to perform a series of backbone modifications with well-known chemistries and investigate some of the effects on polymer reactivity as well as the physical and biological properties of the nanoparticles that can be formed. Additionally, in order to further improve the green credentials of the enzymatic synthesis, a solvent derived from renewable resources, (2-methyl tetrahydrofuran, 2-MeTHF) will be employed, the first time for PGA synthesis, to replace the more traditionally used and fossil-based tetrahydrofuran (THF).^{39–42}

Experimental Section

Materials

Novozym 435 lipase ([9001-62-1], derived from *C. antarctica* (>5000 U/g) and immobilized on an acrylic macroporous resin, was kindly donated by Novozymes A/S, Denmark. Glycerol and all the novel diols (ethylene glycol, PEG400, 1,4-butyne diol, 1,4-butanediol, 1,3-benzodimethanol, 1,6-hexanediol and 2-hydroxyethyl disulfide) were purchased from Sigma–Aldrich UK. Divinyl adipate [4074-90-2] was purchased from TCI America and SPI supplies. All chemicals were used as received. Solvents were purchased from Fischer Scientific UK and used without further purification unless otherwise stated. Water was deionised before use. Solvent evaporation was performed using a rotary evaporator under reduced pressure.

General Methods and Instrumentation

Nuclear Magnetic Resonance Spectroscopy (NMR): Polymer formation and repetitive unit chemical structure assignment were determined using ¹H-NMR spectroscopy. Approximately 4 mg of sample were dissolved in 2 mL of acetone-*d*₆ or CDCl₃ and analysed using a Bruker DPX 400 MHz spectrometer operating at 400 MHz (¹H), assigning chemical shifts in parts per million (ppm). MestReNova 6.0.2 copyright 2009 (Mestrelab Research S. L.) was used for analysing the spectra.

Gel Permeation Chromatography (GPC): was performed in THF (HPLC grade, Fisher Scientific) as the eluent at 40 °C using two Agilent PL-gel mixed-D columns in series, an injection loop of 50 μL, with a flow rate of 1 mL min⁻¹. A differential refractometer (DRI) was

used for the detection of samples (solution containing approximately 4 mg dissolved in 2 mL of THF, filtered in 0.22 μm Teflon filter). The system was calibrated using poly(methyl methacrylate) standards with average molecular weight in the range from 540 to $1.02 \cdot 10^6 \text{ g mol}^{-1}$ and dispersity (\mathcal{D}) close to 1.0

Differential Scanning Calorimetry (DSC): was used to determine the thermal transition of the polymers produced. The analysis was performed on a TA-Q2000 (TA instruments), which was calibrated with indium and sapphire standards under N_2 flow (50 mL min^{-1}). The sample (5-10 mg) was weighed into a T-zero sample pan (TA instruments) with a reference T-zero pan remaining empty. Both lid pans were pin-holed and all samples were heated at a rate of $10 \text{ }^\circ\text{C min}^{-1}$, from $-90 \text{ }^\circ\text{C}$ to $200 \text{ }^\circ\text{C}$. To remove any thermal history of the individual samples two heating cycles were recorded and the second heating cycle was used to determine the glass transition temperature (T_g).

Dynamic Light Scattering (DLS): Particle size analyses were performed by DLS utilizing a Zetasizer Nano spectrometer (Malvern Instruments Ltd) equipped with a 633 nm laser at a fixed angle of 173° . Nanoparticles were prepared at a concentration of 1 mg/mL adopting a simple solvent displacement methodology (acetone/PBS ratio 1:5). Samples were equilibrated at $25 \text{ }^\circ\text{C}$ for 30 seconds prior to measurements. All experiments were performed in duplicate averaging 10 scans per run of the same sample.

Water Contact Angle (θ): Water contact angle (WCA) values were measured at $25 \text{ }^\circ\text{C}$ using a Kruss DSA 100 equipped with dedicated software. Samples were prepared by coating microscopic glass slides with polymer thin films by solvent evaporation of 3 mg/mL polymer solutions in acetone. Six measurements were recorded for each polymer.

“Traditional” and “Greener” PGA Synthesis

PGA was synthesized (Figure 1) by enzymatic polymerization of divinyl adipate (DVA) and glycerol following a protocol adapted from Taresco *et al.*¹³ Glycerol (12.5 mmol) and DVA (12.5 mmol) were poured into a 20 mL glass vial and dissolved into THF (10 mL), or in the greener alternative 2-MeTHF (10 mL). To this mixture, Novozym 435 (0.11 g) was added. The resulting mixture was stirred at 200 rpm with a magnetic stirrer and submerged in an oil bath at $50 \text{ }^\circ\text{C}$ for 1.5 h, 3 h, 5 h or 24 h. A needle was inserted through the rubber septum in order to facilitate the release of acetaldehyde. The removal of this side product favoured the polymerisation process due to the step-growth nature of the process.¹⁹ The reaction was stopped by simply removing the immobilised enzyme by filtration, followed by evaporation of the solvent under reduced pressure. The residual material was kept under vacuum at around $25 \text{ }^\circ\text{C}$ for three days to remove the residual solvent. The resultant highly viscous yellow liquid was stored at $-20 \text{ }^\circ\text{C}$ in order to minimise possible hydrolysis side reactions.

One-Pot PGA Backbone Diol-Alteration Synthesis in 2-MeTHF

PGA-diol was synthesized (Scheme 1) by enzymatic polymerization of divinyl adipate (DVA), glycerol and one of the diols from a protocol adapted from Taresco *et al.*¹³ Glycerol (6.25 mmol) and the selected functionalised diols (6.25 mmol) were added to DVA (12.5 mmol) in a 20 mL glass vial and dissolved into 2-MeTHF (10 mL). In particular, the glycerol moiety was partially replaced by the diols according to the functional groups involved, maintaining a 1:1 stoichiometry molar ratio (considering that only the primary alcohols of glycerol would react in the polycondensation step). To this mixture, Novozym 435 (0.11 g) was added. The resulting mixture was stirred at 200 rpm with a magnetic stirrer and submerged in an oil bath at 50 °C for 3 h. A needle was inserted through the rubber septum in order to facilitate the release of acetaldehyde. The removal of this side product favoured the polymerisation process due to the step-growth nature of the process.¹⁹ The reaction was stopped by simply removing the immobilised enzyme by filtration, followed by evaporation of the solvent under reduced pressure. The residual material was kept under vacuum at around 25 °C for three days to remove the residual solvent. The resultant polymer was stored at -20 °C in order to minimise possible hydrolysis side reactions.

Thiol–ene chemistry of PGA-alkene and PGA-alkyne

The reactivity of the ene- and yne- functionalities introduced in PGA-alkene and PGA-alkyne was probed by a radical thiol–ene reaction with benzyl mercaptan as the model thiol. To this aim, PGA-alkene or PGA-alkyne (15 mg) were dissolved in 100 μL of $\text{DMSO-}d_6$. 2,2-Dimethyl-2-phenyl acetophenone (DMPA) (25 μL aliquot of a 80 mg mL^{-1} solution in $\text{DMSO-}d_6$) and benzyl mercaptan (10 equiv.) were added and the reactions were then irradiated by UV at 365 nm for 120 minutes. A final ^1H NMR spectrum was recorded.

Nanoparticle formation

Nanoparticles were prepared by a nanoprecipitation method.²⁰ Polymers (10 mg) were dissolved in acetone (1 mL). The polymeric solution was then added dropwise to deionised water (10 mL) under constant stirring at 550 rpm. Nanoparticle dispersions were formed through solvent exchange between water and acetone. The final dispersion was then left stirring overnight at room temperature in order to reach complete acetone evaporation, final NPs concentration of 1 mg mL^{-1} .

Coumarin-6 (Cou6) encapsulation study

The encapsulation procedure of Cou-6 was adopted from previous reported protocols.^{43,44} Polymer (10 mg) was dissolved in acetone (1 mL). An aliquot (0.5 mL) of a stock solution of Cou6 (3.21 mM in acetone) was added to the polymer solution. The final acetone solution was added dropwise into deionised water (10 mL) under constant stirring at 550 rpm. The final dispersion was then left stirring overnight at room temperature in order to reach

complete acetone evaporation. Nanoparticles/dye dispersions were finally filtered with a 0.22 μm filter. Cou6 control was formulated in the same way but without the addition of any polymer.

$\Delta A\%$ determination

The absorbance of NPs/dye suspensions was measured by using an UV-vis multi-well plate reader at $\lambda=470$ nm. The apparent-solubility ($\Delta A\%$) value of each formulation was calculated according to the previously developed equation:⁴⁵

where A is the absorbance of the NPs dispersion and A_0 corresponds to the absorbance of the drug formulation in water

Cytotoxicity of polymer formulations

Presto Blue™ cell viability assay was performed to assess the effect of the formulations^{39,46} on primary mouse embryonic fibroblast cells, NIH 3T3 cell line. The cells were grown in Dulbecco's modified eagle medium (DMEM) supplemented with 10% (v/v) foetal calf serum and 1% antibiotics (100 units mL^{-1} penicillin, 100 mg mL^{-1} streptomycin, and 0.25 mg mL^{-1} amphotericin B; Life Technologies). Cells were cultured until they reached 80% confluency and subsequently detached from the culture surface using trypsin/EDTA (0.25%/0.02% w/v), centrifuged at 200 x g for 5 min and resuspended in the culture medium. Cells were seeded in a 48 well plate at a density of 10,000 cells per well and allowed to attach for 24 h before the viability experiments. Formulations were dissolved in a complete medium at a concentration of 100 $\mu\text{g mL}^{-1}$ and 500 μL of each formulation were transferred to the wells containing the cells ($n=4$). Cells were exposed to the formulations for 24 and 48 h. Cells cultured in a complete culture medium only were used as a negative control. After 24 or 48 h, media was removed and cells were then washed twice with warm PBS and 100 μL 10% (v/v) PrestoBlue reagent diluted in phenol red-free medium applied per well for 30 minutes. The resulting fluorescence was measured at 560/600 nm ($\lambda_{\text{ex}}/\lambda_{\text{em}}$). Relative metabolic activity was calculated by setting values from the negative control as 100%.

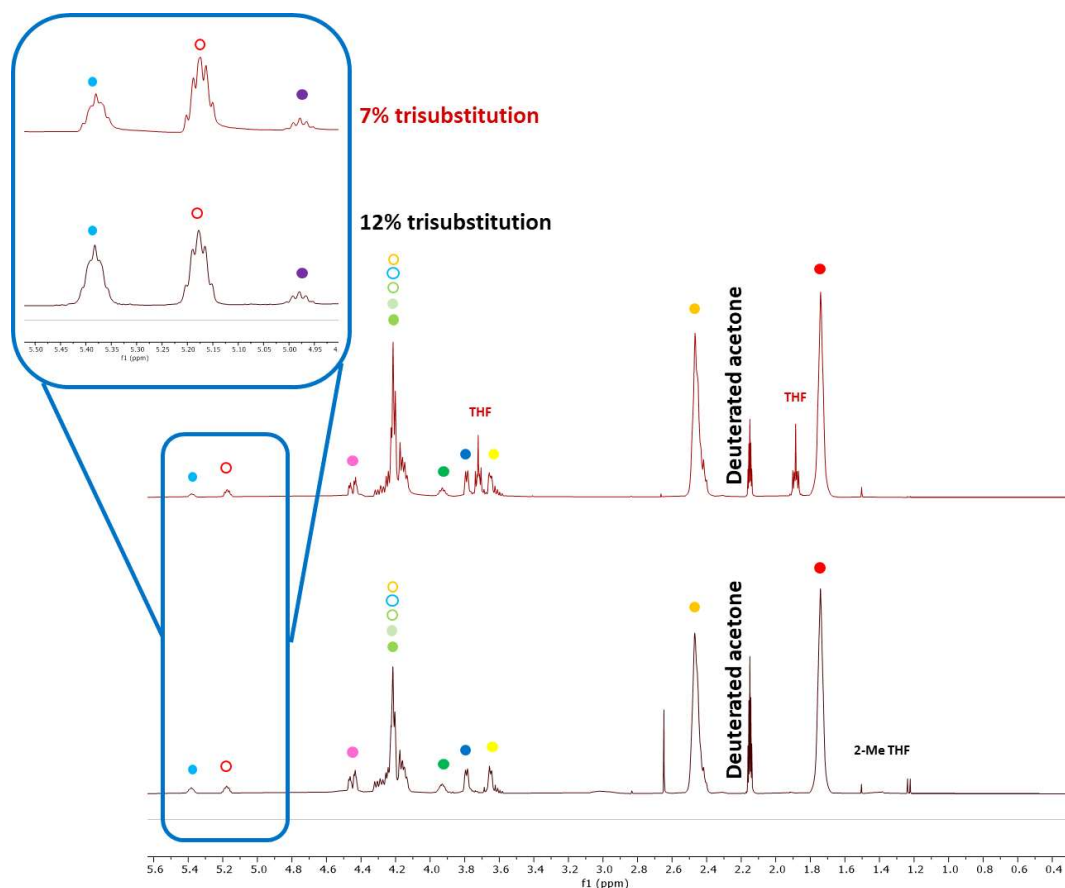
Results and Discussions

Analysis of PGA synthesised in THF and 2-MeTHF and effect of reaction time

PGA was successfully synthesised in both the commonly used THF and 2-MeTHF. This was confirmed by ^1H NMR and GPC analyses. The disappearance of the divinyl peaks at 7.30, 4.87 and 4.59 ppm and change in shape followed by a variation in chemical shift of the glycerol peaks at 4.00 and 4.26 ppm confirmed that the polymerisation occurred (Figure 1

and Figure S1).²⁶





The presence of 1,3-disubstituted (target reaction) 1,2-disubstituted and 1,2,3-trisubstituted glyceride groups (side events) in PGA has been described before, with the latter leading to polymer branching as well as to the decrease of the number of polymer hydroxyl groups.^{47,18,11} However, the 1,2-disubstituted unit, as for the 1,3-disubstituted, provides a

final structure bearing a free hydroxyl group, therefore, it was not considered in the branching calculation. On the other hand, the methine proton from the 1,2,3-trisubstituted glycerol unit at 5.30 ppm (Figure 1, inset) was used to calculate the degree of branching of the PGA polymers,¹³ following a previously reported strategy to calculate the amount of trisubstituted glycerol in PGA.¹³ The integrals of the methine proton at 5.30 ppm and the CH₂ peaks of the adipic repeating units at 1.66 and 2.39 ppm were compared to estimate the degree of branching. In order to evaluate the effects of the solvent on the final polymer architecture, we calculated the degree of branching for each polymer produced in the two solvents. This was found to be *circa* 7 and 12% (Table 1) for PGAs synthesised at 50 °C for 24 h in THF and 2-MeTHF, respectively. In particular, a batch-to-batch variation in 1,2,3-trisubstituted glycerol was observed with a slight increase related to the reaction time (variation from 1 to 3% when increasing the reaction time up to 24h). In addition, the small variation might be due to different degradation events in the two solvents during the screened reaction period, presumably promoted by lipase during long contact times. Indeed, for polymerisations carried out for 5 h, at the same reaction temperature, in each solvent, the degree of branching was found to be similar, 4% (in THF) and 6% (in 2-MeTHF) (Table 1). These preliminary observations confirmed that the adoption of 2-MeTHF as a reaction medium did not significantly affect the molecular weight distribution or the degree of branching, at least for short reaction times. In addition, with the intent of determining the optimum reaction time, further kinetic studies were carried out in this “greener” alternative solvent for 1.5 h and 3 h (at 50 °C). After 1.5 h the degree of branching was only 3%, and the number-average molecular weight of the polymer was lower than the 5 h and 24 h comparisons. In addition to this, the residual vinylic protons from the unreacted DVA or, due to the lower molecular weight, from the end group could be seen at 7.30, 4.87 and 4.59 ppm in the ¹H NMR spectrum (Figure S2). On the other hand, after 3 h, the degree of branching was found to be around 6% and the resulting PGA molecular weight was around 3200 g mol⁻¹ (\mathcal{D} = 2.70). It can be noticed that both the degree of branching and the molecular weight of the polymer after 3 h polymerisation were comparable with those obtained after 5 h polymerisation and for this reason we adopted 3 h as the best compromise between reaction time and conversion in final polymer for all the PGA backbone alteration polymerisations. It is important to mention that the reaction temperature and timing adopted in the present work are within the working window of Novozym 435 lipase previously reported for 2-MeTHF. In fact, it has been demonstrated that Novozym 435, in 2-MeTHF, can successfully catalyse both ring opening polymerisation and polycondensations with temperatures ranging from 30 to 85 °C and for reaction periods over 6h.^{39,42}

Table 1. Number-average molecular weight (M_n), dispersity (\mathcal{D}) and degree of branching of PGAs prepared in THF and 2-MeTHF at different reaction times at 50°C.

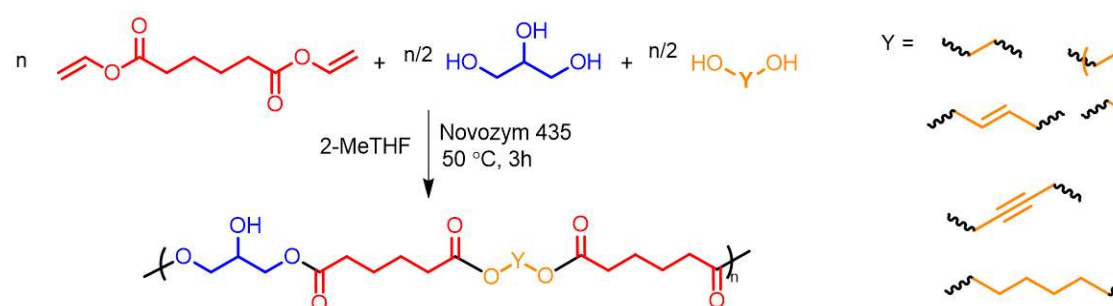
Reaction Media	Reaction time (h)	M_n (g mol ⁻¹) ^{a*}	\mathcal{D} ^{a*}	Degree of branching (%) ^b
THF	24	3000	2.70	~7±2
THF	5	3600	2.80	~4±1
2-MeTHF	24	3000	3.40	~12±3
2-MeTHF	5	3500	2.90	~6±1
2-MeTHF	3	3200	2.70	~6±1
2-MeTHF	1.5	2600	2.10	~3±1

^a Molecular mass determined by GPC at 40 °C, using THF as the mobile phase. ^{a*}Due to the lack of purification,

oligomers peaks can be noticed. These have been taken into account in the total integration. ^b Polymer branching, referred to the 1,2,3-trisubstituted unit, calculated by ¹H NMR analysis (comparison between the integrals of the methine CH peak of trisubstituted glycerol at 5.30 ppm, to that at 1.66 or 2.39 ppm of CH₂CH₂C(O) of adipic acid repeating units). Branching measurements taken out of two different reactions performed in the same conditions.

Synthesis of PGA with different diols in the backbone

The stoichiometric addition of functionalised diols, to replace part of the glycerol, was adopted to investigate the possible range of chemical and physical properties of the final PGA derivatives. Only commercially available diols were selected (Scheme 1) and used without further purifications.



¹H NMR and GPC analyses confirmed that the new functionalities have been integrated into the polymer backbone. In particular, the O-CH₂ diol peak is shifted upon esterification with the adipic moiety (Figure S3) and a general peak broadening was observed (Figure S3, PGA-1,4-butyndiol example). Moreover, the addition of a second diol noticeably decreases the final degree of branching, from *ca.* 6% to 1-4% (Table 2). This is likely due to the decrease in the number of secondary hydroxyl groups that can take part in the branching. Similarly, GPC traces showed a broad ($2.00 \leq D \leq 2.90$) polymeric peak for each derivative, ranging from about M_n 2200 up to 6400 g/mol and traces of oligomers as previously observed for the bare PGA backbone (Figure S3 shows successful modification, further examples are also presented in the SI). The modified PGAs were found to be amorphous materials apart from the 1,6-n-hexanediol variation which showed both a T_g at around -50 °C and a weak melting transition at around 13 °C (DSC analysis of the polymers section in supporting info). This phenomenon might be due to the symmetry between the hexanediol and adipic chains, in fact, when the disulfide group was added no melting transition could be observed. The set of polymers displayed a single glass transition temperature (T_g) in the range of -29 to -50 °C (Table 2); close to the T_g of -28 °C for the original PGA which is usually

a viscous waxy liquid at room temperature. In general, the use of aliphatic alkyl diol (ethylene glycol and hexanediol) improved polymer flexibility with a consequent decrease in T_g with respect to the pure PGA. As expected, the length of the alkyl chain was found to affect polymer T_g . Specifically, PGA-hexanediol showed a lower T_g than PGA-ethylene glycol. Controversially, when PEG400 was used in place of hexanediol we did not observe a further decrease in T_g . Presumably, in this case, the presence of ether groups able to establish H-bonds with the PGA hydroxyl groups, in some ways, reduced the freedom of movement of polymer chains.

The propensity of a drop of water to wet the surface of a material is defined as contact angle of the specific material (θ). The introduction of the functionalised diol substituents will alter the hydrophobic/hydrophilic behaviour. In practice high contact angles corresponding with hydrophobic surfaces, and low angles more hydrophilic surfaces. PGA variants possess experimental θ ranging from *circa* 19 to 70°. In particular, high hydrophilic diols such as PEG400 conferred high hydrophilicity increasing the wettability of the material surface when compared to the pristine PGA (58°) and the other variants, confirming the rearrangement of the hydrophile PEGylated chain towards the water droplet. On the other hand, more hydrophobic moieties like 1,3-benzendimethanol and 1,6-n-hexanediol endowed the final polymers with a hydrophobic property translated in higher contact angles (62.5 to 66.9).

Table 2. Number-average molecular weight (M_n), dispersity (\mathcal{D}), degree of branching, T_g and water contact angle of PGA-derivatives.

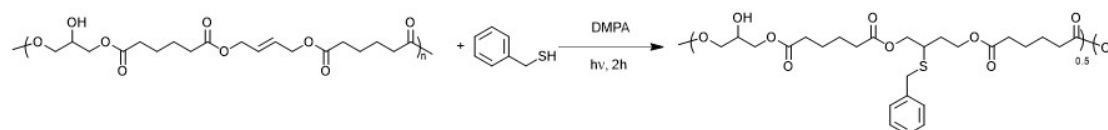
Entry	PGA-modification	Acronyms	M_n (g mol^{-1}) ^{a*}	\mathcal{D} ^{a*}	Degree of branching (%) ^b	T_g (°C) ^c	Water contact angle
1	PGA	PGA	3200	2.90	~6	-28	58.2
2	PGA-ethylene glycol	PGA-EG	2200	2.00	~2	-41	59.3
3	PGA-PEG400	PGA-PEG400	3500	1.70	~2	-50	19.2
4	PGA-1,4-butynediol	PGA-1,4BY	2700	2.10	~2	-30	57.9
5	PGA-1,4-butenediol	PGA-1,4BE	2600	2.60	~3	-47	48.6
6	PGA-1,3-benzendimethanol	PGA-1,3Ph	2500	2.10	~4	-30	62.5
7	PGA-1,6-n-hexanediol	PGA-1,6H	6400	2.00	~3	-50	66.9
8	PGA-2-hydroxyethyl disulfide	PGA-SS	4400	1.65	~2	-38	58.0

^a Molecular mass determined by GPC at 40 °C, using THF as the mobile phase. ^{a*}Due to the lack of purification, oligomers peaks can be noticed. These have been taken into account in the total integration. ^b Polymer branching calculated by ¹H-NMR (comparison between the integrals of the methine CH peak of trisubstituted glycerol at 5.30 ppm, to that at 1.66 or 2.39 ppm of CH₂CH₂C(O) of adipic acid repeating units). ^c Measured by DSC. ^d Measured by Kruss DSA 100.

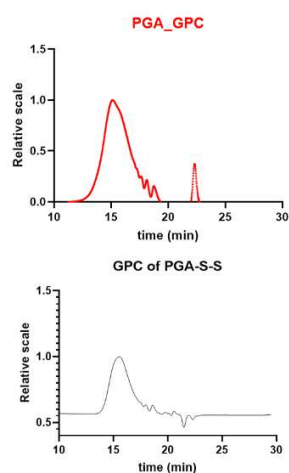
PGA reactive and responsive variations

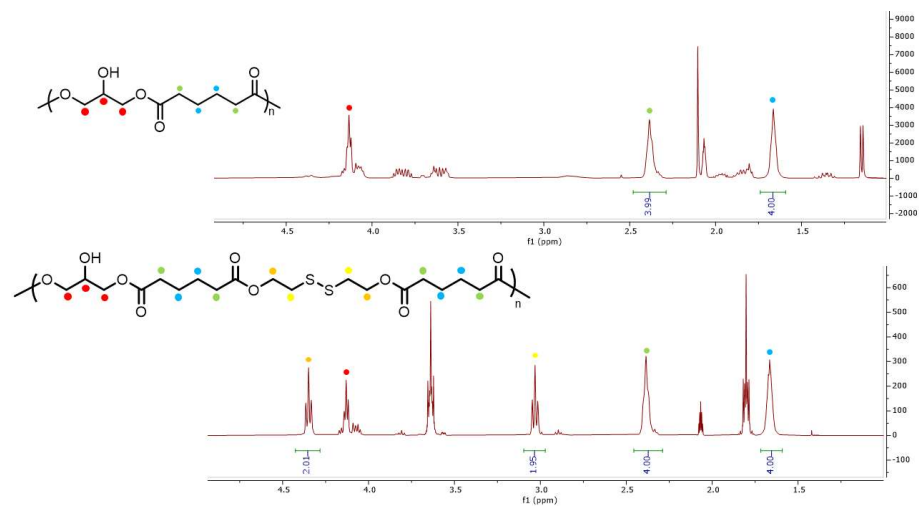
A particular example of modification is the incorporation of alkene and alkyne moieties into the polymer backbone. This can then lead to a highly versatile approach to a variety of additional functionalities by exploiting a series of well-established reaction pathways,

including azide-alkyne cycloadditions and thiol-ene modifications.^{48,49} To prove the reactivity of these ene- and yne- functionalities and to highlight the possibility to endow the PGA backbone with additional properties, we probed the reactivity of the double bond by a radical thiol-ene reaction with benzyl mercaptan as the model thiol (Scheme 2). The macromolecules were reacted with 10 equivalents of the thiol with DMPA as a photoinitiator, followed by irradiation at 365 nm for 120 minutes.^{50,51} The intensity of the resonance related to the alkenyl protons, at 5.9 ppm, reduced by half when compared to the CH_2 peaks of the adipic repeating units at 2.39 ppm (Figure S4).



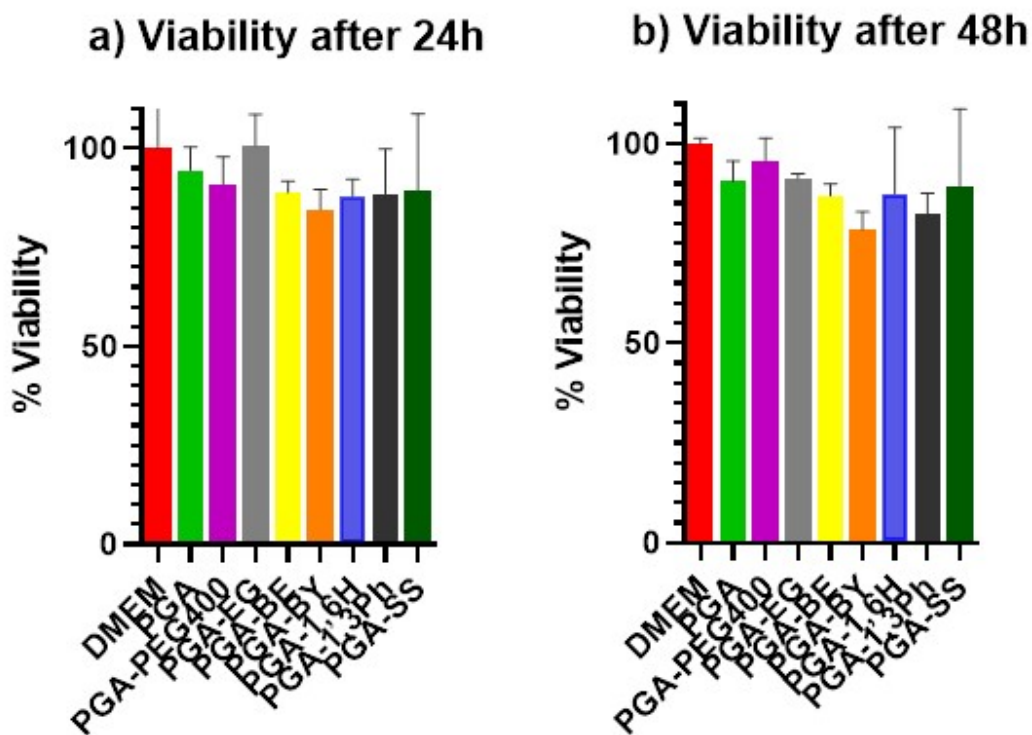
In addition to the abovementioned modifications, we also investigated the insertion of an additional moiety into the backbone to bring additional functionality. 2-Hydroxyethyl disulfide is a readily available and well-known redox-responsive linear diol.^{52,53} As a proof of concept and with the aim of producing a multiresponsive (redox responsive and biodegradable) polymer in a straightforward synthetic pathway, we substituted 1,6-n-hexanediol with 2-hydroxyethyl disulfide. The incorporation of this diol was successful as confirmed by 1H NMR and GPC (Figure 2). In addition, the polymer can self-assemble in water producing NPs with sizes around 115 nm and PDI of 0.08. This modification may provide interesting opportunities in the future as a smart multiresponsive polymeric platform for drug delivery applications.





Polymer Cytotoxicity

These novel materials show potential for pharmaceutical and more specifically for drug delivery applications, so an initial assessment of their *in vitro* toxicity on NIH 3T3 model cell line was conducted. Cytocompatibility tests of the modified PGAs resuspended in cell culture aqueous medium at a fixed concentration of $100 \mu\text{g mL}^{-1}$ showed no significant *in vitro* cytotoxicity; no decrease in cellular metabolic activity over 24-48 h on the cell type studied (Figure 3a and 3b). One should bear in mind that in accordance with ISO 10993-5:2009⁵⁴ if the cell viability is greater than or equal to 70% in relation to control group (100% viability) the polymer material can be considered non-cytotoxic.



Self-assembling ability of hydrophilic/hydrophobic PGA variants

Amphiphilic balancing to tune polymer self-assembly and interaction with small molecules was achieved in the synthesized PGA variants by incorporating a range of hydrophilic and hydrophobic moieties into the polymer backbone. In the nanoprecipitation step the different modified PGAs self-assembled in water into nanoaggregates, with diameters ranging from *ca.* 88 nm up to 120 nm and very narrow particle size distributions exhibiting PDI equal or below 0.1 (Figure 4A, Table 3). PGA-ethylene glycol showed similar size and PDI values of the bare PGA, hinting at a minimal effect on the final self-assembling behaviour of the short diol chain. While both the 1,6-n-hexanediol and PEG400 PGA variations gave small NPs (around 88 and 92 nm, respectively) the two modifications provided opposite hydrophobic/hydrophilic behaviours from their contact angle values. This highlights the importance of the amphiphilic modification of the repeating unit. On the other hand, the incorporation of a bulky aromatic ring, in the case of PGA-1,3-benzenedimethanol, led to an increase of around 15 nm of the hydrodynamic size of the final NPs compared to the bare PGA (Table 3).

Table 3. Size and PDI of empty and Cou6 loaded nanoparticles.^a

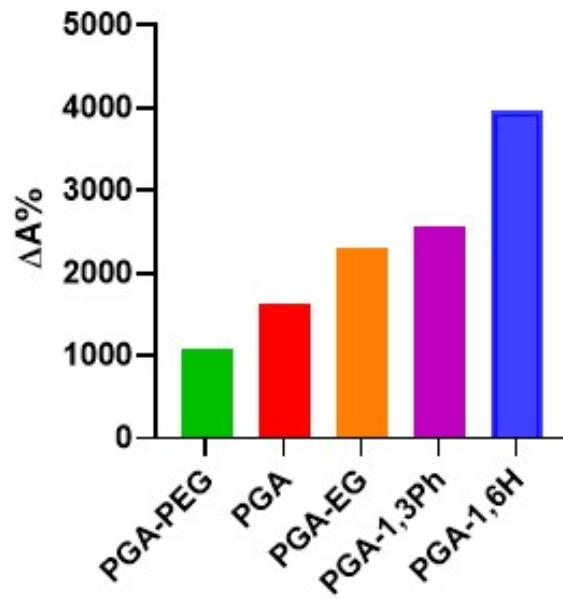
PGA-modification	Empty nanoparticles		Cou6 loaded nanoparticles	
	Average size (nm)	PDI	Average size (nm)	PDI
PGA	102.8 ± 4	0.104 ± 0.01	92.2 ± 2	0.031 ± 0.01
PGA-EG	108.6 ± 2	0.077 ± 0.01	105.5 ± 2	0.045 ± 0.01
PGA-PEG400	92.1 ± 1	0.102 ± 0.01	272.3 ± 3	0.397 ± 0.07
PGA-1,3Ph	117.6 ± 1	0.079 ± 0.01	93.46 ± 2	0.131 ± 0.03
PGA-1,6H	87.5 ± 2	0.052 ± 0.03	87.5 ± 1	0.098 ± 0.01

^a All data were produced by DLS measurements.

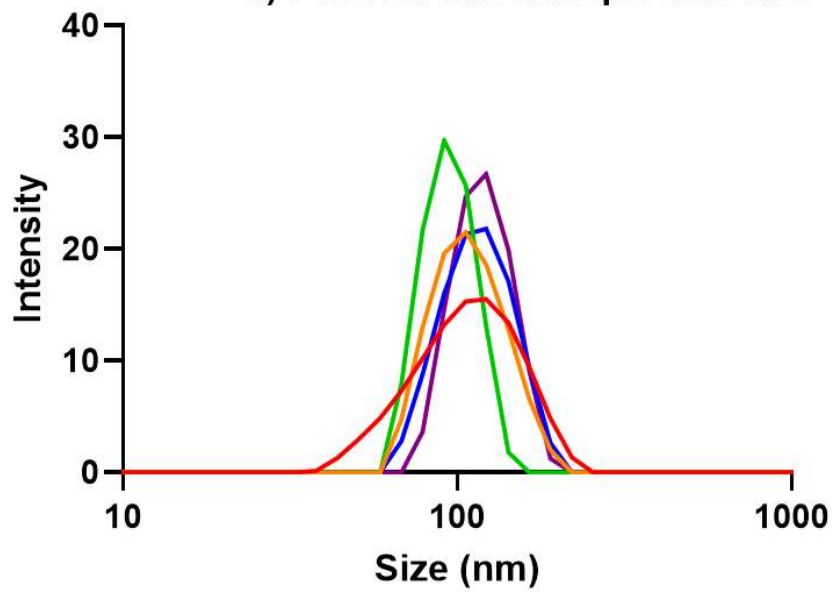
Coumarin6 enhancing solubility in an aqueous environment.

To prove the encapsulation ability of the novel PGA-variants, the highly hydrophobic Coumarin-6 (Cou6) fluorescent dye was used as a model. Cou6 is a water-insoluble small molecule that can be used as a model to mimic the behaviour of lipophilic drugs for initial evaluation of drug delivery- and drug release experiments. Cou6 was co-nanoprecipitated in water with and without (control) PGA modifications. In order to quickly rank the polymers in terms of Cou6 apparent-solubility enhancement, $\Delta A\%$ values were calculated (Figure 4b).

b) Polymer ranking



a) PGA variant nanoparticle size



PEG400, showed the lowest $\Delta A\%$ likely due to a shorter hydrophobic counterpart in the repetitive unit compared to the rest of the library. PGA-EG and PGA-1,3Ph, instead, showed higher $\Delta A\%$ (2292 and 2566, respectively) and therefore a higher ability to solubilise/encapsulate Cou6 when compared to PGA (1633) and PGA-PEG400 (1075). This is likely because of the increased hydrophobicity portion in the repetitive units able to interact with the small model dye. However, the aromatic modification, despite a higher hydrophobicity contribution compared to the other modifications, did not show a remarkable dye interaction, possibly due to the bulkiness of the ring. The aromatic ring might reduce the space available inside the hydrophobic core of the nanoaggregates for the Cou6. On the other hand, PGA-1,6-H $\Delta A\%$ was around 4000, almost 2.5 times higher than that of the bare PGA. The addition of the 1,6-n-hexanediol moiety seemed to be a perfect balance of amphiphilicity, chain length and chain flexibility which allowed for self-assembling of well-defined NPs as well as providing an improvement of the apparent solubility in water of Cou6.

Conclusions

We have demonstrated that it is possible to alter the chemical composition of the PGA backbone by utilising a small library of functionalised/functionalisable diols with a straightforward one-pot synthetic modification of the common enzymatic pathway. The selected diols introduce additional chemical handles, such as double/triple bonds, PEGylated chains and aromatic rings, directly into the backbone of PGA. In addition, tuning of the PGA amphiphilic polymer backbone was demonstrated by adding a series of diols with different hydrophilic/hydrophobic behaviours. The reactivity of the ene-PGA variants was probed by a simple UV activated thiol-ene reaction. Self-assembly and the encapsulation of a water-insoluble model molecule were demonstrated to be directly related to the nature of the added functionalised diol. Furthermore, *in vitro* cell-viability assays demonstrated that the produced PGA variants are nontoxic and may be considered appropriate vehicles for future investigation as drug delivery carriers. In addition, in order to enhance the green credentials of the enzymatic synthesis, a solvent derived from renewable resources, (2-methyl tetrahydrofuran, 2-MeTHF) was employed for the synthesis of all the PGA-variants as replacement of the more traditionally used and fossil-based

tetrahydrofuran (THF).

ACKNOWLEDGMENTS

PLJ was supported by the Engineering and Physical Sciences Research Council and SFI Centre for Doctoral Training in Sustainable Chemistry [grant number EP/S02236/1]. LRC and RW were supported by the Engineering and Physical Sciences Research Council [grant numbers EP/P031684/1]. E.A.A. wishes to gratefully acknowledge the Swiss National Science Foundation (SNSF) (P2FRP2_184280). We thank Mark Guyler (University of Nottingham) for his technical support with all the laboratory equipment. We are indebted to Shaz Aslam and Kevin Butler for their technical input to analysis by NMR spectroscopy.

References

- (1) Lim, C.; Lin, A. L.; Zhao, H. Metabolic Strategies for Microbial Glycerol Overproduction. *J. Chem. Technol. Biotechnol.* **2018**, *93* (3), 624–628. <https://doi.org/10.1002/jctb.5465>.
- (2) Quispe, C. A. G.; Coronado, C. J. R.; Carvalho, J. A. Glycerol: Production, Consumption, Prices, Characterization and New Trends in Combustion. *Renewable Sustainable Energy Rev.* **2013**, *27* (October), 475–493. <https://doi.org/10.1016/j.rser.2013.06.017>.
- (3) Lochab, B.; Varma, I. K.; Bijwea, J. Sustainable Polymers Derived From Naturally Occurring Materials. *Adv. Mater. Phys. Chem.* **2012**, *02* (04), 221–225. <https://doi.org/10.4236/ampc.2012.24B056>.
- (4) Chong, C. C.; Aqsha, A.; Ayoub, M.; Sajid, M.; Abdullah, A. Z.; Yusup, S.; Abdullah, B. A Review over the Role of Catalysts for Selective Short-Chain Polyglycerol Production from Biodiesel Derived Waste Glycerol. *Environ. Technol. Innov.* **2020**, *19*, 100859. <https://doi.org/10.1016/j.eti.2020.100859>.
- (5) Gandini, A.; Lacerda, T. M. From Monomers to Polymers from Renewable Resources: Recent Advances. *Prog. Polym. Sci.* **2015**, *48*, 1–39. <https://doi.org/10.1016/j.progpolymsci.2014.11.002>.
- (6) Perin, G. B.; Felisberti, M. I. Enzymatic Synthesis of Poly(Glycerol Sebacate): Kinetics, Chain Growth, and Branching Behavior. *Macromolecules* **2020**, *53* (18), 7925–7935. <https://doi.org/10.1021/acs.macromol.0c01709>.
- (7) Luman, N. R.; Smeds, K. A.; Grinstaff, M. W. The Convergent Synthesis of Poly(Glycerol-Succinic Acid) Dendritic Macromolecules. *Chem. – A Eur. J.* **2003**, *9* (22), 5618–5626. <https://doi.org/https://doi.org/10.1002/chem.200305172>.
- (8) Zamboulis, A.; Nakiou, E. A.; Christodoulou, E.; Bikiaris, D. N.; Kontonasaki, E.; Liverani, L.; Boccaccini, A. R. Polyglycerol Hyperbranched Polyesters: Synthesis, Properties and Pharmaceutical and Biomedical Applications. *Int. J. Mol. Sci.* **2019**, *20*

- (24). <https://doi.org/10.3390/ijms20246210>.
- (9) Valerio, O.; Misra, M.; Mohanty, A. K. Poly(Glycerol- Co-Diacids) Polyesters: From Glycerol Biorefinery to Sustainable Engineering Applications, A Review. *ACS Sustainable Chemistry and Engineering*. American Chemical Society May 7, 2018, pp 5681–5693. <https://doi.org/10.1021/acssuschemeng.7b04837>.
- (10) Lang, K.; Sánchez-Leija, R. J.; Gross, R. A.; Linhardt, R. J. Review on the Impact of Polyols on the Properties of Bio-Based Polyesters. *Polymers (Basel)*. **2020**, *12* (12). <https://doi.org/10.3390/polym12122969>.
- (11) Uyama, H.; Inada, K.; Kobayashi, S. Regioselectivity Control in Lipase-Catalyzed Polymerization of Divinyl Sebacate and Triols. *Macromol. Biosci*. **2001**, *1* (1), 40–44. [https://doi.org/10.1002/1616-5195\(200101\)1:1<40::AID-MABI40>3.0.CO;2-T](https://doi.org/10.1002/1616-5195(200101)1:1<40::AID-MABI40>3.0.CO;2-T).
- (12) Shoda, S.; Uyama, H.; Kadokawa, J.; Kimura, S.; Kobayashi, S. Enzymes as Green Catalysts for Precision Macromolecular Synthesis. *Chem. Rev*. **2016**, *116* (4), 2307–2413. <https://doi.org/10.1021/acs.chemrev.5b00472>.
- (13) Taresco, V.; Creasey, R. G.; Kennon, J.; Mantovani, G.; Alexander, C.; Burley, J. C.; Garnett, M. C. Variation in Structure and Properties of Poly(Glycerol Adipate) via Control of Chain Branching during Enzymatic Synthesis. *Polymer* **2016**, *89*, 41–49. <https://doi.org/10.1016/j.polymer.2016.02.036>.
- (14) Naolou, T.; Meister, A.; Schöps, R.; Pietzsch, M.; Kressler, J. Synthesis and Characterization of Graft Copolymers Able to Form Polymersomes and Worm-like Aggregates. *Soft Matter* **2013**, *9* (43), 10364–10372. <https://doi.org/10.1039/c3sm51716k>.
- (15) Alaneed, R.; Golitsyn, Y.; Hauenschild, T.; Pietzsch, M.; Reichert, D.; Kressler, J. Network Formation by Aza-Michael Addition of Primary Amines to Vinyl End Groups of Enzymatically Synthesized Poly(Glycerol Adipate). *Polym. Int*. **2021**, *70* (1), 135–144. <https://doi.org/10.1002/pi.6102>.
- (16) Swainson, S. M. E.; Styliari, I. D.; Taresco, V.; Garnett, M. C. Poly (Glycerol Adipate) (PGA), an Enzymatically Synthesized Functionalizable Polyester and Versatile Drug Delivery Carrier: A Literature Update. *Polymers (Basel)*. **2019**, *11* (10). <https://doi.org/10.3390/polym11101561>.
- (17) Weiss, V. M.; Lucas, H.; Mueller, T.; Chytil, P.; Etrych, T.; Naolou, T.; Kressler, J.; Mäder, K. Intended and Unintended Targeting of Polymeric Nanocarriers: The Case of Modified Poly(Glycerol Adipate) Nanoparticles. *Macromol. Biosci*. **2018**, *18* (1), 1700240. <https://doi.org/10.1002/mabi.201700240>.
- (18) Kline, B. J.; Beckman, E. J.; Russell, A. J. One-Step Biocatalytic Synthesis of Linear Polyesters with Pendant Hydroxyl Groups. *J. Am. Chem. Soc*. **1998**, *120* (37), 9475–9480. <https://doi.org/10.1021/ja9808907>.
- (19) Kallinteri, P.; Higgins, S.; Hutcheon, G. A.; St. Pourçain, C. B.; Garnett, M. C. Novel Functionalized Biodegradable Polymers for Nanoparticle Drug Delivery Systems. *Biomacromolecules* **2005**, *6* (4), 1885–1894. <https://doi.org/10.1021/bm049200j>.
- (20) Swainson, S. M. E.; Taresco, V.; Pearce, A. K.; Clapp, L. H.; Ager, B.; McAllister, M.; Bosquillon, C.; Garnett, M. C. Exploring the Enzymatic Degradation of Poly(Glycerol

- Adipate). *Eur. J. Pharm. Biopharm.* **2019**, *142* (July), 377–386.
<https://doi.org/10.1016/j.ejpb.2019.07.015>.
- (21) Abd-El-Aziz, A. S.; Antonietti, M.; Barner-Kowollik, C.; Binder, W. H.; Böker, A.; Boyer, C.; Buchmeiser, M. R.; Cheng, S. Z. D.; D'Agosto, F.; Floudas, G.; Frey, H.; Galli, G.; Genzer, J.; Hartmann, L.; Hoogenboom, R.; Ishizone, T.; Kaplan, D. L.; Leclerc, M.; Lendlein, A.; Liu, B.; Long, T. E.; Ludwigs, S.; Lutz, J. F.; Matyjaszewski, K.; Meier, M. A. R.; Müllen, K.; Müllner, M.; Rieger, B.; Russell, T. P.; Savin, D. A.; Schlüter, A. D.; Schubert, U. S.; Seiffert, S.; Severing, K.; Soares, J. B. P.; Staffilani, M.; Sumerlin, B. S.; Sun, Y.; Tang, B. Z.; Tang, C.; Théato, P.; Tirelli, N.; Tsui, O. K. C.; Unterlass, M. M.; Vana, P.; Voit, B.; Vyazovkin, S.; Weder, C.; Wiesner, U.; Wong, W. Y.; Wu, C.; Yagci, Y.; Yuan, J.; Zhang, G. The Next 100 Years of Polymer Science. *Macromol. Chem. Phys.* **2020**, *221* (16), 1–22. <https://doi.org/10.1002/macp.202000216>.
- (22) Gordhan, D.; Swainson, S. M. E.; Pearce, A. K.; Styliari, I. D.; Lovato, T.; Burley, J. C.; Garnett, M. C.; Taresco, V. Poly (Glycerol Adipate): From a Functionalized Nanocarrier to a Polymeric-Prodrug Matrix to Create Amorphous Solid Dispersions. *J. Pharm. Sci.* **2020**, *109* (3), 1347–1355. <https://doi.org/10.1016/j.xphs.2019.12.004>.
- (23) Suksiriworapong, J.; Taresco, V.; Ivanov, D. P.; Styliari, I. D.; Sakchaisri, K.; Junyaprasert, V. B.; Garnett, M. C. Synthesis and Properties of a Biodegradable Polymer-Drug Conjugate: Methotrexate-Poly(Glycerol Adipate). *Colloids Surfaces B Biointerfaces* **2018**, *167*, 115–125. <https://doi.org/10.1016/j.colsurfb.2018.03.048>.
- (24) Tchoryk, A.; Taresco, V.; Argent, R.; Ashford, M. B.; Gellert, P.; Stolnik, S.; Grabowska, A. M.; Garnett, M. C. Penetration and Uptake of Nanoparticles in 3D Tumour Spheroids. *Bioconjug. Chem.* **2019**, acs.bioconjchem.9b00136. <https://doi.org/10.1021/acs.bioconjchem.9b00136>.
- (25) Animasawun, R. K.; Taresco, V.; Swainson, S. M. E.; Suksiriworapong, J.; Suksiriworapong, J.; Walker, D. A.; Garnett, M. C. Screening and Matching Polymers with Drugs to Improve Drug Incorporation and Retention in Nanoparticles. *Mol. Pharm.* **2020**, *17* (6), 2083–2098. <https://doi.org/10.1021/acs.molpharmaceut.0c00236>.
- (26) Taresco, V.; Suksiriworapong, J.; Creasey, R.; Burley, J. C.; Mantovani, G.; Alexander, C.; Treacher, K.; Booth, J.; Garnett, M. C. Properties of Acyl Modified Poly(Glycerol-Adipate) Comb-like Polymers and Their Self-Assembly into Nanoparticles. *J. Polym. Sci. Part A Polym. Chem.* **2016**, *54* (20), 3267–3278. <https://doi.org/10.1002/pola.28215>.
- (27) Wersig, T.; Hacker, M. C.; Kressler, J.; Mäder, K. Poly(Glycerol Adipate) – Indomethacin Drug Conjugates – Synthesis and in Vitro Characterization. *Int. J. Pharm.* **2017**, *531* (1), 225–234. <https://doi.org/10.1016/j.ijpharm.2017.08.093>.
- (28) Alaneed, R.; Hauenschild, T.; Mäder, K.; Pietzsch, M.; Kressler, J. Conjugation of Amine-Functionalized Polyesters With Dimethylcasein Using Microbial Transglutaminase. *J. Pharm. Sci.* **2020**, *109* (2), 981–991. <https://doi.org/10.1016/j.xphs.2019.10.052>.
- (29) Steiner, J.; Alaneed, R.; Kressler, J.; Mäder, K. Fatty Acid-Modified Poly(Glycerol Adipate) Microparticles for Controlled Drug Delivery. *J. Drug Deliv. Sci. Technol.* **2021**, *61*, 102206. <https://doi.org/https://doi.org/10.1016/j.jddst.2020.102206>.

- (30) Taresco, V.; Suksiriworapong, J.; Styliari, I. D.; Argent, R. H.; Swainson, S. M. E.; Booth, J.; Turpin, E.; Laughton, C. A.; Burley, J. C.; Alexander, C.; Garnett, M. C. New N-Acyl Amino Acid-Functionalized Biodegradable Polyesters for Pharmaceutical and Biomedical Applications. *RSC Adv.* **2016**, *6* (111), 109401–109405. <https://doi.org/10.1039/C6RA21464A>.
- (31) Styliari, I. D.; Conte, C.; Pearce, A. K.; Hüsler, A.; Cavanagh, R. J.; Limo, M. J.; Gordhan, D.; Nieto-Orellana, A.; Suksiriworapong, J.; Couturaud, B.; Williams, P.; Hook, A. L.; Alexander, M. R.; Garnett, M. C.; Alexander, C.; Burley, J. C.; Taresco, V. High-Throughput Miniaturized Screening of Nanoparticle Formation via Inkjet Printing. *Macromol. Mater. Eng.* **2018**, *303* (8), 1–9. <https://doi.org/10.1002/mame.201800146>.
- (32) Weiss, V. M.; Naolou, T.; Hause, G.; Kuntsche, J.; Kressler, J.; Mäder, K. Poly(Glycerol Adipate)-Fatty Acid Esters as Versatile Nanocarriers: From Nanocubes over Ellipsoids to Nanospheres. *J. Control. Release* **2012**, *158* (1), 156–164. <https://doi.org/10.1016/j.jconrel.2011.09.077>.
- (33) Weiss, V. M.; Naolou, T.; Amado, E.; Busse, K.; Mäder, K.; Kressler, J. Formation of Structured Polygonal Nanoparticles by Phase-Separated Comb-like Polymers. *Macromol. Rapid Commun.* **2012**, *33* (1), 35–40. <https://doi.org/10.1002/marc.201100565>.
- (34) Jbeily, M.; Naolou, T.; Bilal, M.; Amado, E.; Kressler, J. Enzymatically Synthesized Polyesters with Pendent OH Groups as Macroinitiators for the Preparation of Well-Defined Graft Copolymers by Atom Transfer Radical Polymerization. *Polym. Int.* **2014**, *63* (5), 894–901. <https://doi.org/10.1002/pi.4676>.
- (35) Tawfeek, H.; Khidr, S.; Samy, E.; Ahmed, S.; Murphy, M.; Mohammed, A.; Shabir, A.; Hutcheon, G.; Saleem, I. Poly(Glycerol Adipate-Co- Ω -Pentadecalactone) Spray-Dried Microparticles as Sustained Release Carriers for Pulmonary Delivery. *Pharm. Res.* **2011**, *28* (9), 2086–2097. <https://doi.org/10.1007/s11095-011-0433-6>.
- (36) Kunda, N. K.; Alfagih, I. M.; Dennison, S. R.; Tawfeek, H. M.; Somavarapu, S.; Hutcheon, G. A.; Saleem, I. Y. Bovine Serum Albumin Adsorbed PGA-CO-PDL Nanocarriers for Vaccine Delivery via Dry Powder Inhalation. *Pharm. Res.* **2015**, *32* (4), 1341–1353. <https://doi.org/10.1007/s11095-014-1538-5>.
- (37) Mohamed, A.; Kunda, N. K.; Ross, K.; Hutcheon, G. A.; Saleem, I. Y. Polymeric Nanoparticles for the Delivery of MiRNA to Treat Chronic Obstructive Pulmonary Disease (COPD). *Eur. J. Pharm. Biopharm.* **2019**, *136*, 1–8. <https://doi.org/10.1016/j.ejpb.2019.01.002>.
- (38) Rodrigues, T. C.; Oliveira, M. L. S.; Soares-Schanoski, A.; Chavez-Rico, S. L.; Figueiredo, D. B.; Gonçalves, V. M.; Ferreira, D. M.; Kunda, N. K.; Saleem, I. Y.; Miyaji, E. N. Mucosal Immunization with PspA (Pneumococcal Surface Protein A)-Adsorbed Nanoparticles Targeting the Lungs for Protection against Pneumococcal Infection. *PLoS One* **2018**, *13* (1), e0191692. <https://doi.org/10.1371/journal.pone.0191692>.
- (39) Englezou, G.; Kortsen, K.; Pacheco, A. A. C.; Cavanagh, R.; Lentz, J. C.; Krumins, E.; Sanders-Velez, C.; Howdle, S. M.; Nedoma, A. J.; Taresco, V. 2-Methyltetrahydrofuran (2-MeTHF) as a Versatile Green Solvent for the Synthesis of Amphiphilic Copolymers via ROP, FRP, and RAFT Tandem Polymerizations. *J. Polym. Sci. (Hoboken, NJ, U. S.)*

- 2020, 58 (11), 1571–1581. <https://doi.org/10.1002/pol.20200183>.
- (40) Ielo, L.; Miele, M.; Pillari, V.; Senatore, R.; Mirabile, S.; Gitto, R.; Holzer, W.; Alcántara, A. R.; Pace, V. Taking Advantage of Lithium Monohalocarbenoid Intrinsic α -Elimination in 2-MeTHF: Controlled Epoxide Ring-Opening En Route to Halohydrins. *Org. Biomol. Chem.* **2021**. <https://doi.org/10.1039/D0OB02407D>.
- (41) Pace, V.; Hoyos, P.; Castoldi, L.; Domínguez De María, P.; Alcántara, A. R. 2-Methyltetrahydrofuran (2-MeTHF): A Biomass-Derived Solvent with Broad Application in Organic Chemistry. *ChemSusChem*. John Wiley & Sons, Ltd August 2012, pp 1369–1379. <https://doi.org/10.1002/cssc.201100780>.
- (42) Pellis, A.; Byrne, F. P.; Sherwood, J.; Vastano, M.; Comerford, J. W.; Farmer, T. J. Safer Bio-Based Solvents to Replace Toluene and Tetrahydrofuran for the Biocatalyzed Synthesis of Polyesters. *Green Chem.* **2019**, 21 (7), 1686–1694. <https://doi.org/10.1039/c8gc03567a>.
- (43) Curia, S.; Howdle, S. M. Towards Sustainable Polymeric Nano-Carriers and Surfactants: Facile Low Temperature Enzymatic Synthesis of Bio-Based Amphiphilic Copolymers in ScCO₂. *Polym. Chem.* **2016**, 7 (11), 2130–2142. <https://doi.org/10.1039/c6py00066e>.
- (44) Rivolta, I.; Panariti, A.; Lettiero, B.; Sesana, S.; Gasco, P.; Gasco, M. R.; Masserini, M.; Miserocchi, G. Cellular Uptake of Coumarin-6 as a Model Drug Loaded in Solid Lipid Nanoparticles. *J. Physiol. Pharmacol. an Off. J. Polish Physiol. Soc.* **2011**, 62 (1), 45–53.
- (45) Sanna, M.; Sicilia, G.; Alazzo, A.; Singh, N.; Musumeci, F.; Schenone, S.; Spriggs, K. A.; Burley, J. C.; Garnett, M. C.; Taresco, V.; Alexander, C. Water Solubility Enhancement of Pyrazolo[3,4- d] Pyrimidine Derivatives via Miniaturized Polymer-Drug Microarrays. *ACS Med. Chem. Lett.* **2018**, 9 (3), 193–197. <https://doi.org/10.1021/acsmchemlett.7b00456>.
- (46) Kolbuk, D.; Jeznach, O.; Wrzecionek, M.; Gadomska-Gajadur, A. Poly(Glycerol Succinate) as an Eco-Friendly Component of PLLA and PLCL Fibres towards Medical Applications. *Polymers (Basel)*. **2020**, 12 (8). <https://doi.org/10.3390/POLYM12081731>.
- (47) Naolou, T.; Hussain, H.; Baleed, S.; Busse, K.; Lechner, B.-D.; Kressler, J. The Behavior of Fatty Acid Modified Poly(Glycerol Adipate) at the Air/Water Interface. *Colloids Surfaces A Physicochem. Eng. Asp.* **2015**, 468, 22–30. <https://doi.org/https://doi.org/10.1016/j.colsurfa.2014.12.003>.
- (48) Summonte, S.; Racaniello, G. F.; Lopodota, A.; Denora, N.; Bernkop-Schnürch, A. Thiolated Polymeric Hydrogels for Biomedical Application: Cross-Linking Mechanisms. *J. Control. Release* **2021**, 330, 470–482. <https://doi.org/https://doi.org/10.1016/j.jconrel.2020.12.037>.
- (49) Kim, E.; Koo, H. Biomedical Applications of Copper-Free Click Chemistry: In Vitro{,} in Vivo{,} and Ex Vivo. *Chem. Sci.* **2019**, 10 (34), 7835–7851. <https://doi.org/10.1039/C9SC03368H>.
- (50) Francini, N.; Purdie, L.; Alexander, C.; Mantovani, G.; Spain, S. G. Multifunctional Poly[N-(2-Hydroxypropyl)Methacrylamide] Copolymers via Postpolymerization

- Modification and Sequential Thiol-Ene Chemistry. *Macromolecules* **2015**, *48* (9), 2857–2863. <https://doi.org/10.1021/acs.macromol.5b00447>.
- (51) Sun, L.; Pitto-Barry, A.; Thomas, A. W.; Inam, M.; Doncom, K.; Dove, A. P.; O'Reilly, R. K. Core Functionalization of Semi-Crystalline Polymeric Cylindrical Nanoparticles Using Photo-Initiated Thiol-Ene Radical Reactions. *Polym. Chem.* **2016**, *7* (13), 2337–2341. <https://doi.org/10.1039/c5py01970b>.
- (52) Deng, B.; Ma, P.; Xie, Y. Reduction-Sensitive Polymeric Nanocarriers in Cancer Therapy: A Comprehensive Review. *Nanoscale* **2015**, *7* (30), 12773–12795. <https://doi.org/10.1039/C5NR02878G>.
- (53) Monteiro, P. F.; Travanut, A.; Conte, C.; Alexander, C. Reduction-Responsive Polymers for Drug Delivery in Cancer Therapy—Is There Anything New to Discover? *WIREs Nanomedicine and Nanobiotechnology* **2021**, *13* (2), e1678. <https://doi.org/https://doi.org/10.1002/wnan.1678>.
- (54) Standardization), I. (the I. O. for. ISO 10993-5:2009(en) Biological evaluation of medical devices — Part 5: Tests for in vitro cytotoxicity.